Journal of Computational Neuroscience 5, 171–190 (1998)

Analysis and Neural Network Modeling of the Nonlinear Correlates of Habituation in the Vestibulo-ocular Reflex

ERNST R. DOW
Center for Biophysics and Computational Biology and Beckman Institute, University of Illinois at Urbana/Champaign, Urbana, IL 61801
edow@uiuc.edu

THOMAS J. ANASTASIO
Center for Biophysics and Computational Biology, Department of Molecular and Integrative Physiology, and Beckman Institute, University of Illinois at Urbana/Champaign, Urbana, IL 61801
tstasio@uiuc.edu

Received February 11, 1997; Revised August 19, 1997; Accepted October 31, 1997

Action Editor: A. Georgopoulos

Abstract. Through the process of habituation, continued exposure to low-frequency (0.01 Hz) rotation in the dark produced suppression of the low-frequency response of the vestibulo-ocular reflex (VOR) in goldfish. The response did not decay gradually, as might be expected from an error-driven learning process, but displayed several nonlinear and nonstationary features. They included asymmetrical response suppression, magnitude-dependent suppression for lower- but not higher-magnitude head rotations, and abrupt-onset suppressions suggestive of a switching mechanism. Microinjection of lidocaine into the vestibulocerebellum of habituated goldfish resulted in a temporary dishabituation. This suggests that the vestibulocerebellum mediates habituation, presumably through Purkinje cell inhibition of vestibular nuclei neurons. The habituated VOR data were simulated with a feed-forward, nonlinear neural network model of the VOR in which only Purkinje cell inhibition of vestibular nuclei neurons was varied. The model suggests that Purkinje cell inhibition may switch in to introduce nonstationarities, and cause asymmetry and magnitude-dependency in the VOR to emerge from the essential nonlinearity of vestibular nuclei neurons.

Keywords: learning, plasticity, goldfish, VOR, cerebellum

Introduction

The function of the vestibulo-ocular reflex (VOR) is to rotate the eyes to maintain retinal image stability during head rotation (Wilson and Melvill Jones, 1979). If not for these compensatory eye movements, vision would be blurred, making it impossible for an animal to move and see simultaneously. The VOR is mediated by interneurons found in the vestibular nuclei in the brainstem. Vestibular nuclei neurons receive and process head rotation signals from vestibular sensory afferents and send eye rotation commands to the motoneurons of the eye muscles. At higher frequencies of rotation, the VOR appears to operate as a time-invariant and linear system. However, through the process of habituation, continued exposure to low-frequency rotation can cause a time-variant suppression of the VOR, and this suppression can in turn cause the VOR to exhibit nonlinear behavior. The purpose of this article is to gain insight into the neural mechanisms of the VOR

through analysis and modeling of the nonlinear and nonstationary correlates of VOR habituation.

Under normal circumstances, the VOR is exposed to a broad spectrum of frequencies of head rotation that are mostly higher than about 1 Hz (Grossman et al., 1988). In the laboratory, continued exposure in the dark to higher-frequency (>0.1 Hz) head rotations appears to have little effect on the gain of the VOR. However, exposure in the dark either to continued sinusoidal head rotation at low-frequency or to repeated transient head rotations produces suppression of the VOR in rabbits, rats, cats, monkeys, and humans (for a review, see Schmid and Jeannerod, 1985). This process is known as VOR habituation. The VOR suppression due to habituation can be characterized as a decrease in VOR gain (eye velocity/head velocity).

Previous experimental work has suggested that habituation may be correlated with nonlinear behavior in the VOR. In a recent study (Dow and Anastasio, 1996), low-frequency VOR gain in habituated goldfish was found to increase 20 times when a low-frequency head rotation was combined with higher-frequency rotation. This finding demonstrated that the VOR in habituated goldfish fails to obey the principle of superposition, which is a fundamental property of linear systems. Also, repeated unilateral transient rotations in the dark can cause a unilateral habituation, resulting in an asymmetrical VOR response in the cat (Crampton, 1962; Collins and Updegraff, 1965; Mertens and Collins, 1967; Jeannerod et al., 1981; Clément et al., 1981) and dog (Collins and Updegraff, 1965). Asymmetries have also been observed in the rat VOR as it habituated to continued sinusoidal rotation at low frequency (Tempia et al., 1991).

Regions of the vestibulocerebellum known as the nodulus and uvula may mediate habituation. Ablation of the nodulus and uvula in habituated cats (Singleton, 1967; Torte et al., 1994) and monkeys (Waespe et al., 1985; Cohen et al., 1992a) produces dishabituation of the VOR. Also, cerebellectomy dishabituates the goldfish VOR (Dow and Anastasio, 1996). Electrical stimulation of the nodulus during head rotations caused a temporary cessation of the VOR response in the cat (Fernández and Fredrickson, 1964) and monkey (Solomon and Cohen, 1994). Although the responses of vestibular afferents do not appear to habituate (Proctor and Fernández, 1963; Courjon et al., 1987), the responses of vestibular nuclei neurons have been observed to decrease with repeated transient rotations (Kileny et al., 1980). These studies demonstrate the involvement of the vestibulocerebellum in habituation and suggest that habituation could be mediated by cerebellar Purkinje cell inhibition of vestibular nuclei neurons.

The purpose of this study was to explore the nonlinear and nonstationary aspects of VOR habituation in goldfish. Goldfish were chosen because they have a robust VOR and show a greater degree of VOR plasticity than other animals studied to date (Schairer and Bennett, 1986; Pastor et al., 1992; Weissenstein et al., 1996; Dow and Anastasio, 1996). One hour of exposure to 0.01 Hz rotation in the dark was sufficient to reduce VOR gain at that frequency by 20 times. However, habituation was minimal with exposure to higher-frequency rotation (>0.1 Hz) for the same duration. Analysis of time-series data revealed several nonlinear and nonstationary features in the VOR of habituating goldfish, including response asymmetries and abrupt-onset response reductions. Injection of lidocaine into the vestibulocerebellum of habituated goldfish resulted in temporary dishabituation, suggesting that habituation is mediated by the vestibulocerebellum, perhaps through inhibition of vestibular nuclei neurons by Purkinje cells. The nonlinear properties of the VOR response in habituating goldfish were reproduced using a simple, nonlinear neural network model of the VOR in which only the level of Purkinje cell inhibition of vestibular nuclei neurons was varied.

Our experimental results suggest that VOR habituation in the goldfish involves a nonstationary suppression of the VOR by the vestibulocerebellum during head rotation at low but not high frequency, and this suppression can cause the VOR to exhibit nonlinear behavior. The VOR is nonlinear, as any neural system must be, and our modeling results suggest that its apparent linear operation under certain circumstances is an emergent property of its network organization. However, circumstances that alter this organization, such as those that induce habituation, can reveal the essentially nonlinear nature of the VOR.

Methods

Experimental Animals

All experiments were performed on comet goldfish (*carassius auratus*), 10 to 15 cm in length, that were either purchased locally or from a fishery (Ozark Fish Hatcheries, Stoughtlin, MO). The goldfish were kept in freshwater aquaria and maintained at a temperature of 18°C, with alternating 12 h periods of light and

dark. The horizontal VOR was tested in naïve goldfish and in goldfish during and after exposure that had been exposed to long-duration head rotations at various frequencies. The VOR was also tested in goldfish during electrical stimulation of, or lidocaine injection into, the vestibulocerebellum. Stimulation and injection sites were verified histologically.

Experimental Preparation

Before every experiment, each goldfish was wrapped in gauze and was restrained horizontally underwater, using contoured body supports, in a 10 l, cylindrical, experimental tank. The gauze and body supports held the goldfish snugly without trauma and also covered the lateral line organs, thus preventing their stimulation by water flow, which was minimal in the cylindrical tank (see below). The head of the goldfish was centered within the experimental tank. Its mouth was opened over a plastic tube and secured to it with string to immobilize the head. Aquarium water was continuously recirculated through the tube to respire the goldfish. To measure eye movements, a small coil of Teflon-insulated copper wire (5.3 mm external coil diameter) was attached to the tough outer covering of the left eye using ophthalmic suture. Procedures for recording the goldfish VOR are similar to those described previously (Pastor et al., 1992).

To prepare the goldfish for electrical stimulation or lidocaine injection experiments, they were first anesthetized by immersion for 30 to 60 min in a separate tank with dissolved Tricaine methane-sulfonate (MS-222, Sigma) at 60 mg/l. They were then transferred to and restrained in the experimental tank, where they remained anesthetized for approximately 30 min. A 4 mm $\times$ 6 mm section of skull superior and slightly rostral to the cerebellum was immediately elevated by first scraping away the skin with a dental tool and then cutting the perimeter with a drill. To further immobilize the head for the longer-duration electrical stimulation experiments, an area of skull rostral to the cavity was exposed, grooves were cut with a drill, and one end of a metal rod was secured to the skull with dental cement (Ketac-Cem, Espe, Germany). The other end of the rod was coupled to the experimental tank. The water level in the experimental tank was adjusted to prevent water from flowing into the skull cavity. The surfaces of the optic tectum and cerebellum were exposed by aspirating from the cavity the gelatinous fluid that surrounds the brain in the goldfish. A tank-mounted micromanipulator, carrying an electrode or a pipette, was zeroed by positioning either tip at the midline on the rostral surface of the cerebellum, about 1 mm superior to the junction with the optic tectum, and then retracting the tip. In order to maintain the environment around the brain, the skull cavity was then filled with agar or, more commonly, an aerated mixture of mineral oil and white petrolatum.

Electrical Stimulations

To stimulate electrically, a tungsten microelectrode (0.5 MΩ, Micro Probe, Inc., Clarksburg, MD) was inserted into the vestibulocerebellum by returning the tip to the 0 position (see above) and advancing it 2.2 or 2.3 mm, depending on the size of the goldfish, at a 40 deg angle to the horizontal. The VOR was recorded before and after microelectrode insertion, and the integrity of the response was verified before the electrical stimulations were made. Electrical stimulation consisted of a 2 to 10 s train of bipolar current pulses, 1 ms in width, delivered at a rate of 200/s, that ranged in amplitude from $\pm$10 to $\pm$70 μA (biphasic pulse generator and stimulus isolator, BAK Electronics, Inc., Germantown, MD). After the last stimulation an electrolytic lesion was made at the site with a 3 min train of unipolar (5 ms, 1 mA) current pulses delivered at a rate of 4/s.

Lidocaine Injections

A glass micropipette was inserted into the vestibulocerebellum using the same semistereotaxic procedure described above for the stimulating electrodes. The VOR was tested to verify that it was not affected by insertion of the micropipette. The micropipette was filled with a solution of 2% lidocaine and alcian blue dye (both from Sigma) dissolved in goldfish saline. After the goldfish had habituated to low-frequency head rotation (0.01 Hz for 1 h), 250 nl of lidocaine solution was injected with a syringe attached to the micropipette. The micropipette was immediately withdrawn following the injection. Data were recorded from the goldfish for up to 2.5 h postinjection as the effects peaked and then wore off.

Histology

After the electrical stimulation or lidocaine injection experiments, the goldfish were immediately reanesthetized and perfused with saline followed by formalin. The brain was removed from the skull, embedded

in egg yolk, cut in 50 μm sections, mounted on slides, and stained with neutral red. Histological material was examined and photographed under light microscopy. All surgical procedures were approved under University of Illinois LACAC protocol number B3R085.

Rotational Stimulation and Eye Movement Recording

To test the horizontal VOR, the experimental tank was mounted on the horizontal platform of a servo-driven rotator (40 ft/1b, Trio-Tech International, San Fernando, CA). The head of the goldfish, and the center of the cylindrical tank, were centered on the vertical axis of rotation. This minimized both centrifugal (that is, linear) acceleration of the head, and water flow in the tank, during rotation. A magnetic field generating frame and demodulator (Remmel Labs, Ashland, MA) was also mounted on the rotating platform, and eye position was transduced using the magnetic search coil technique (Robinson, 1963; Remmel, 1984). Each eye coil was calibrated immediately following the experiment to 0.1 deg at 7 angles that covered the range of eye movement ($\pm$30 deg). The rotator assembly was located inside a Faraday cage and, to ensure that the goldfish received no visual feedback during experiments, the room lights were extinguished and both the cage and the rotator assembly were covered with black mylar shrouds. Platform rotation occurred at discrete frequencies ranging from 0.01 to 1.0 Hz. Habituation was studied at 0.01, 0.1, and 1.0 Hz, but some other frequencies in the range were also tested. Peak velocities were 60 deg/s at all frequencies. Stimuli at this magnitude are considered to be in the linear range for the goldfish VOR (Pastor et al., 1992; Weissenstein et al., 1996). Platform rotation produced nystagmus, which consisted of slow-phase (VOR) and fast-phase (resetting) eye rotations. The eye position and rotator tachometer (head velocity) signals were digitized with a 12 bit AD at 300 Hz for 1 Hz rotations, and at 50 Hz for all other frequencies of rotation, after antialias filtering (eight-pole Butterworth) at half the sampling rate.

Data Analysis and Modeling

Data were analyzed on a computer using programs developed in MATLAB (The Mathworks, Inc., Natick, MA). An optimal digital differentiation routine, which contributed practically 0 amplitude or phase error (Bahill and McDonald, 1983), was used to compute

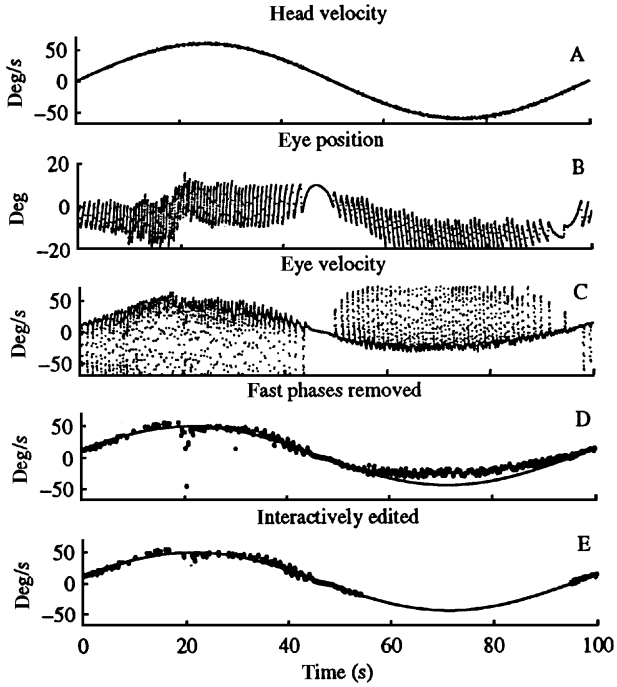

Figure 1. Sinusoidal responses in a naïve goldfish at 0.01 Hz. A: The head velocity trace is shown inverted in this and all subsequent figures to facilitate comparisons to the eye velocity traces. B: The eye position record is digitally differentiated to compute eye velocity (C). D: A computer algorithm removed most of the fast phases, but a few points had to be removed interactively (for example, E: $t = 20$ and 30 s). These traces illustrate an example of a unilateral habituation in which the response in the temporal direction was attenuated (in this and all subsequent figures, positive deflections correspond to the nasally directed positions or velocities of the left eye). To make the best linear estimate of naïve VOR response parameters, the nonsinusoidal portion of the temporal response was removed interactively, and a least square sinusoid was fit to the remaining data. The curve fit to the interactively edited data (E) is reproduced in D for comparison. In order not to obscure the fitted curves, the data in D and E are plotted with thicker points.

eye velocity from eye position (Fig. 1). Fast-phases were removed automatically by a computer algorithm. In some cases final adjustments were made interactively by removing fast-phase data that were not detected by the automatic routine. Additionally, since low-frequency habituation often proceeded asymmetrically during the first cycle of rotation, the habituated portion was edited out so that the amplitude of the naïve slow-phase response could be estimated more accurately (compare Figs. 1D and 1E). Least-squares sinusoids were fit to the edited eye velocity and head velocity records. At least 1 and up to 60 cycles of the response were fit at any frequency. Gain (peak eye velocity/peak head velocity) and phase difference

(eye velocity phase-inverted/head velocity phase) were calculated from the best-fit sinusoids.

Due to the presence of a few extreme values, the median rather than the mean was used as a measure of central tendency, and the semi-interquartile interval (SII) provided the associated measure of variability. Significance was tested nonparametrically with a two-tail Mann-Whitney U test. To analyze the nonlinear characteristics of the data, *xy* plots were constructed by plotting eye velocity against head velocity for one cycle of sinusoidal data, after the records were shifted in time so as to minimize the phase difference between them. The nonlinear features of the data were simulated using a neural network model of the VOR.

Results

Forty-two comet goldfish (*carassius auratus*) provided useful data. The time course of VOR habituation at 0.01 Hz was studied in 28 goldfish. Gain before and after was estimated in 12 of the 28 to measure the amount of VOR habituation at 0.01 Hz. Three goldfish each were used to measure habituation at 0.1 and 1.0 Hz. Recordings were made from the left eye only in most goldfish, but in three of the goldfish recordings were made from both eyes. Four goldfish each were used for the electrical stimulation and lidocaine injection experiments. Twelve of the goldfish were retested at various intervals to measure dishabituation. Some low-frequency VOR habituation data were taken from goldfish used in a previous study of VOR combined-frequency responses (Dow and Anastasio, 1996).

Habituation can produce a suppression of the VOR response at a particular frequency following prolonged rotation at that frequency. To test habituation, goldfish were rotated at a habituating frequency (0.01, 0.1, or 1.0 Hz) for 1 h. This study focused on VOR responses in goldfish habituated at 0.01 Hz because habituation at that frequency was the most effective. One hour of rotation at 0.01 Hz was sufficient to severely reduce VOR response amplitude at this frequency (see below). Spontaneous eye movements were similar in naïve and habituated goldfish.

Analysis of Gain

Least-square sinusoids were fit to the slow-phase eye velocity (*ev*) and head velocity (*hv*) records (see Methods). Gain (*ev* amplitude/*hv* amplitude) and phase difference (*ev* phase-inverted − *hv* phase) at each frequency were computed from the best-fit sinusoids. VOR gain and phase were estimated in naïve goldfish at 0.01, 0.1, and 1.0 Hz. Median gains were 0.42 ± 0.15, 0.45 ± 0.11, and 0.65 ± 0.17, respectively.

Habituation at 0.01 Hz severely reduced VOR gain that frequency but did not affect gain at 0.1 or 1.0 Hz high frequencies. Median gain at 0.01 Hz (the habituating frequency) decreased 21 times, from 0.42 ± 0.15 to 0.020 ± 0.010 in naïve and habituated goldfish, respectively. This difference was highly statistically significant ($p < 0.0001$). Gains at 0.1 Hz and 1.0 Hz were very similar in naïve goldfish and in goldfish habituated at 0.01 Hz, and none of the differences were significant ($p > 0.1$ in all cases). Habituation at 0.01 Hz also produced time- and frequency-dependent changes in VOR phase. Consideration of these phase changes and analysis of habituated VOR dynamics in general are beyond the focus of this article.

Three naïve goldfish each were exposed for 1 h to sinusoidal rotation at 0.1 Hz and 1.0 Hz, and the amount of change in gain at the habituating frequency was measured. At 0.1 Hz, median VOR gain decreased by 1.3 ± 0.017 times and the difference was significant ($p < 0.05$), while that at 1.0 Hz actually increased by 1.2 ± 0.13 times, but the difference was not significant. In comparison, exposure for at least 1 h to 0.01 Hz rotation reduced median gain at the habituating frequency by 21 times (see above). These results indicate that VOR habituation is a phenomenon that is selective for low-frequency rotation. Lack of habituation at higher frequencies of rotation (above $\sim$0.1 Hz) has also been reported in the goldfish (Dow and Anastasio, 1996), rabbit (Ito et al., 1974; Kleinschmidt and Collewijn, 1975), and monkey (Buettner et al., 1981; Jäger and Henn, 1981a).

Process of Habituation

Habituation of the goldfish VOR occurred in various, unpredictable ways and almost always proceeded at different rates for the two directions of eye rotation—nasal and temporal. Note that these directions of eye rotation refer to the left eye, the eye from which most of the recordings were made. Recordings in some goldfish were made from both eyes, and in these it was observed that asymmetrical habituation was conjugate in the sense that when it occurred in the nasal direction for the left eye it occurred in the temporal direction for the right eye and vice-versa. This follows from the fact that the VOR produces conjugate eye movements and

therefore can be studied by observing the movements of only one eye.

Time series for three low frequency (0.01 Hz) runs are shown in Fig. 2. All runs show the initial low-frequency response starting within the first cycle. Positive and negative deflections correspond respectively to nasal and temporal eye velocities. Head velocity (inverted) is shown for comparison. The VOR response of goldfish 112 was strong initially and first-cycle gain was 0.76. Response amplitude began decreasing first in the nasal direction, with an associated baseline shift in the temporal direction. The amplitude of the nasal response fell abruptly in the third cycle. The nasal response in subsequent cycles had a smaller amplitude but also showed abrupt decreases near the nasal peak. Such abrupt decreases in response amplitude were another common feature of VOR habituation in goldfish and produce figure-eight xy plots (see below and Fig. 3C). The amplitude of the temporal VOR response began to decrease after the fourth cycle and continued to habituate gradually throughout the rest of the trace. Such an asymmetrical habituation can occur first to either side and produces a crescent-shaped xy plot (see below and Figs. 3D and 3E).

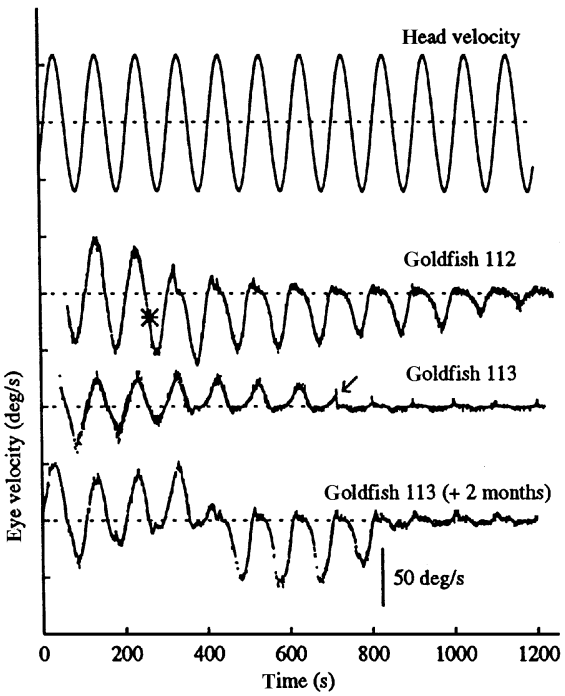

Figure 2. Progress of VOR habituation in two goldfish at 0.01 Hz rotation, showing asymmetries and abrupt transitions. The VOR of goldfish 112 initially habituates in the nasal direction, with a baseline shift in the opposite (temporal) direction. Eye velocity drops on the third cycle with an abrupt transition at the nasal peak ($t = 325$ s). The temporal response habituates more gradually. (The asterisk is for comparison with Fig. 3C.) The VOR of goldfish 113 habituates first in the temporal direction and then in the nasal. Eye velocity drops at about $t = 725$ s with an abrupt transition at the nasal peak (arrow). Thereafter, the only consistent response is a nib at the nasal peak. The last trace shows the VOR of goldfish 113, two months after habituation. There is an immediate rehabituation in the temporal direction with a baseline shift in the nasal direction. A reversal occurs at $t = 400$ s in which the temporal response is dishabituated and the nasal response becomes rehabituated. The dashed line in all traces shows 0 velocity.

Goldfish 113 showed an initial decrease in the amplitude of the temporal VOR response, which was almost completely habituated by the fourth cycle. This temporal habituation may have been accompanied by a slight nasal baseline shift. The amplitude of the nasal response began to fall after the fourth cycle with an abrupt decrease in the seventh cycle (arrow). Starting at 800 s, the nasal response consisted only of small peaks that replaced what would have been the entire nasal response half-cycle. This magnitude-dependent type of response produces a dead-zone xy plot (see below and Figs. 3B and 4). Goldfish 113 was retested after two months, and its initial VOR response was strong, indicating that dishabituation had taken place (see below). The response began rehabituating first in the temporal direction, accompanied by a baseline shift in the nasal direction. The temporal response was almost completely rehabituated after the first four cycles. However, at 400 s, the previously dishabituated nasal response abruptly rehabituated, and the temporal response dishabituated. The temporal response again abruptly rehabituated after four cycles.

The time series show that habituation does not proceed smoothly and symmetrically. An exponential decrease in VOR amplitude would have been expected on the assumption that the habituation process uses some measure proportional to error to drive VOR gain to 0 at low frequency. Instead, the data show asymmetries and abrupt response reductions and reversals that are not consistent with a simple, error-driven learning hypothesis for VOR habituation. Further consideration of habituation as an adaptive process is beyond the focus of this article. Considered here are the VOR nonlinearities and nonstationarities that are associated with habituation.

Time-invariant (that is, static) departures from a linear relationship between the input to the VOR (head velocity) and its output (eye velocity) are considered

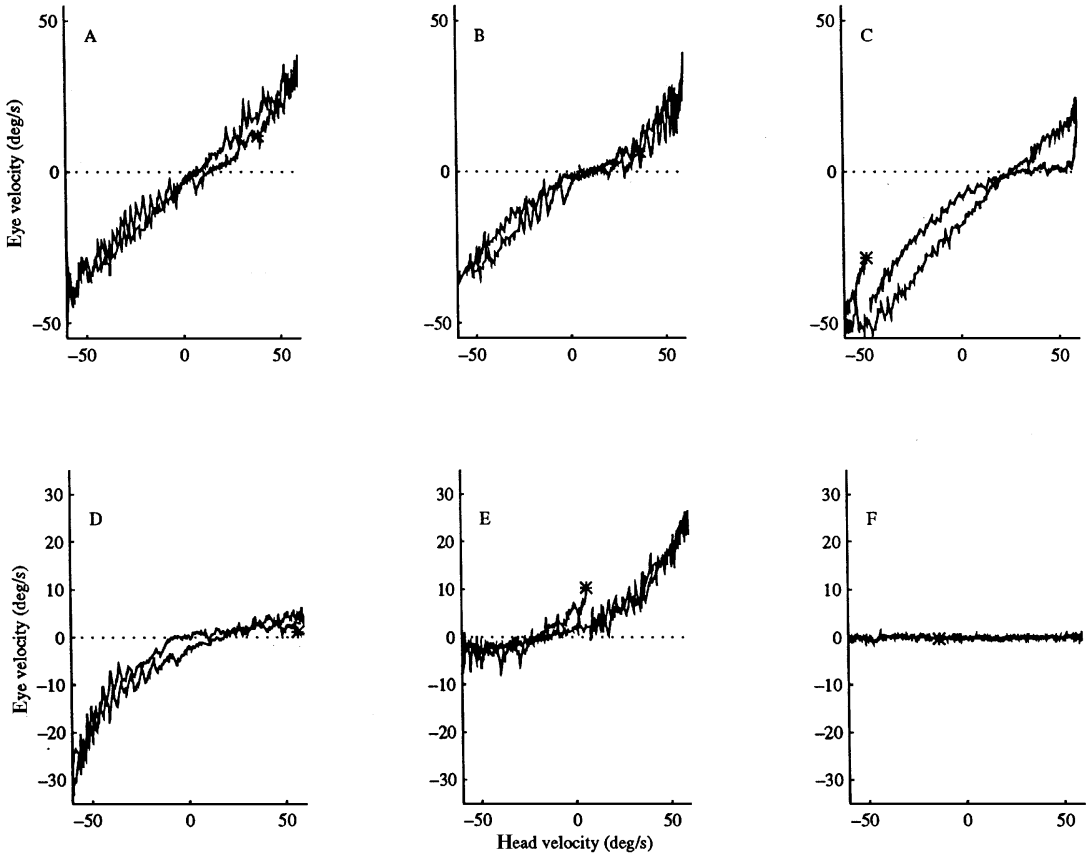

Figure 3. The *xy* plots illustrating some nonlinear and nonstationary features of the VOR in habituating goldfish. All plots show one cycle of the VOR response to head rotation at 0.01 Hz. Eye velocity was plotted against head velocity after the records were shifted in time to minimize any phase difference. The beginning of each cycle is marked by an asterisk, which is most evident in C and E. Data are from different goldfish and illustrate the various types of *xy* plot profiles observed. A: Example of an almost linear response, as observed in some naïve goldfish. B: Soft dead-zone nonlinearity in which the response is attenuated for lower but not higher-magnitude portions of the stimulus cycle. C: Figure-eight *xy* plot due to an abrupt reduction in gain occurring within the cycle. The data in this plot are the same as in Fig. 2, goldfish 112, starting at the asterisk, in which an abrupt (that is, nonstationary) gain reduction takes place at the nasal peak. D: Crescent nonlinearity due to soft rectification in the nasal direction. E: Crescent due to soft rectification in the temporal direction. F: Essentially flat response showing complete habituation in both directions. (Ordinate is expanded in D to F.)

nonlinear. Time-variant changes in that input and output relationship are considered nonstationary. Habituation is a nonstationary process by definition, but this article is concerned with relatively short-term phenomena that take place within one cycle of sinusoidal input. It would be difficult to distinguish nonlinear from nonstationary behavior given only VOR input and output data. However, analysis and modeling will show that these habituated VOR behaviors may be distinguished and explained.

The time-series data reveal several nonlinearities and nonstationarities associated with the process of VOR habituation in goldfish. These features may be described as asymmetrical or abrupt decreases in amplitude and shifts in baseline. These grossly nonstationary and nonlinear responses occurred during continuous, unchanging stimulation at a magnitude well within what would be considered as the linear range of the goldfish VOR (Pastor et al., 1992; Weissenstein et al., 1996). Parameters such as amplitude, phase, and baseline—which characterize the purely sinusoidal responses of stationary, linear systems—begin to lose their meaning when applied to the nonstationary, nonlinear VOR responses observed during and after habituation in goldfish. To better characterize these nonlinear and nonstationary properties, *xy* plots of individual cycles of the habituating goldfish VOR responses were constructed.

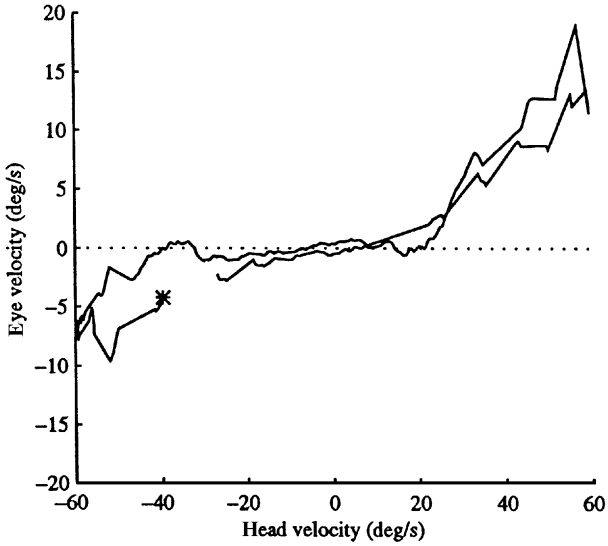

Figure 4. The *xy* plot of a soft dead-zone nonlinearity at 0.03 Hz. This type of nonlinearity was often observed with habituation at 0.01 Hz but was more pronounced at slightly higher frequencies (0.03 and 0.05 Hz). The asterisk indicates the start of the cycle. The soft dead-zone *xy* profile is characteristic of the magnitude-dependent VOR response.

xy Plots

To construct an *xy* plot from sinusoidal data, one cycle of eye velocity was plotted against head velocity after the records were shifted in time to minimize the phase difference between them. A similar procedure has been used to characterize the nonlinear response properties of semicircular canal afferents in the bullfrog (Segal and Outerbridge, 1982a, 1982b). The *xy* plots characterized the nonlinear and nonstationary properties of the response. Several distinct *xy* profiles emerged from the analysis that corresponded to the features observed in the time series. These *xy* plots are shown in Fig. 3 (0.01 Hz) and Fig. 4 (0.03 Hz).

An example of the *xy* plot of a linear, stationary VOR response at 0.01 Hz is shown in Fig. 3A. Such a response was sometimes observed in naïve goldfish that did not begin habituating during the initial cycle of 0.01 Hz rotation. It was close to being perfectly sinusoidal, so that (phase-adjusted) eye and head velocity increased and decreased together over the entire cycle. This produced an *xy* plot that was nearly a straight line. However, the *xy* trajectory in Fig. 3A is slightly open. This opening was due to a small amount of skew in the response, which caused the excursions to and from baseline for each half-cycle to occur at slightly different rates. Few goldfish showed such a linear response, even on the first cycle. More typically, the naïve VOR response at 0.01 Hz produced an *xy* plot that can be described as a soft dead-zone nonlinearity. This type of *xy* plot is characteristic of a magnitude-dependent response that is stronger for the higher than for the lower magnitude portions of the stimulus cycle. It can be contrasted with a hard dead-zone in which the response is 0 for the lower-magnitude portions. An example of a soft dead-zone *xy* plot is shown in Fig. 3B.

An example of the *xy* plot of a nonstationary VOR response is shown in C. The data in this figure corresponds to the third cycle of the habituating response of goldfish 112 shown in Fig. 2 (asterisks mark the beginning of this cycle both in the time series of Fig. 2 for goldfish 112 and in the *xy* plot of Fig. 3C). This response cycle was somewhat asymmetrical, but the most salient feature of the time series (Fig. 2) was an abrupt decrease in the amplitude of the response that occurs at the nasal peak. This abrupt transition produced a discontinuity in the nasal part of the *xy* trajectory (Fig. 3C). The trajectory crossed itself once, near zero eye velocity, forming a figure-eight. The gradual decrease in the temporal response produced a separation of the beginning and ending points that occurs in the temporal part of the trajectory. Such a separation would be produced by any change that occurred during the cycle that caused the beginning and ending values to differ. Asymmetry in the response cycle plotted in Fig. 3C caused the *xy* trajectory to have a curved appearance. This is illustrated more clearly for the more stationary asymmetrical response cycles shown as *xy* plots in Figs. 3D and 3E.

The *xy* trajectory shown in Fig. 3D is crescent-shaped. The VOR response from which this plot was generated had habituated more strongly in the nasal direction. This crescent shaped *xy* trajectory can be described as a soft rectification in which the response in the rectified direction is small but nonzero. It can be contrasted with a hard rectification in which the response in the rectified direction is 0. The small amount of opening in the *xy* plot reflects some skew in the response, but the trajectory begins and ends at the same value indicating that the response is relatively stationary. The *xy* trajectory shown in Fig. 3E also shows a crescent shape but, in contrast to Fig. 3D, the VOR response from which this plot was generated had habituated more strongly in the temporal direction. Whether the goldfish habituated first to the nasal or temporal side was not related to the initial direction of rotation. The *xy* trajectory in Fig. 3E begins and ends at different values, suggesting some nonstationarity in

the response. However, changes in the response that occurred during this cycle appear to have been gradual rather than abrupt.

The *xy* plots shown in Figs. 3A through 3E were constructed from VOR data taken relatively early on in the habituation process, after less than 0.5 h of rotation at the habituating frequency (0.01 Hz). Goldfish were exposed to rotation at the habituating frequency for at least 1 h. An example of an *xy* plot constructed from data recorded after more than 1 h of habituation is shown in Fig. 3F. The response in both the nasal and temporal directions was essentially flat. Note that the ordinate scales for Figs. 3D, 3E, and 3F are the same, but these are expanded relative to those for Figs. 3A, 3B, and 3C. VOR gain for the cycle of data plotted in Fig. 3F was estimated to be 0.0033.

The soft dead-zone nonlinearity, an example of which is shown in Fig. 3B for stimulation at the habituating frequency (0.01 Hz), was often more pronounced at slightly higher frequencies. A soft dead-zone *xy* plot is chacteristic of a magnitude-dependent response, which is stronger for the higher than for the lower-magnitude portions of the stimulus cycle. Figure 4 shows an example of a soft dead-zone *xy* plot for a goldfish VOR response at 0.03 Hz. The VOR only responded to higher-magnitude head rotations. The response was almost flat for lower-magnitude head rotations. The trajectory is also open, suggesting some skew in the response.

The *xy* plot analysis indicates that the VOR response in habituating goldfish was highly nonlinear and nonstationary. It would be difficult, if not impossible, to describe these responses using parameters such as amplitude, phase, and baseline, which can describe the purely sinusoidal responses of stationary, linear systems. However, the *xy* plot analysis revealed several distinct profiles that can characterize the nonlinear and nonstationary responses of the habituating goldfish VOR. These include the soft-dead zone, crescent (soft-rectification), and figure-eight *xy* profiles. A neural network model that reproduces these nonlinear results is presented in an upcoming section.

Dishabituation and Spontaneous Nystagmus

The effects of VOR habituation in the dark have been observed to persist over a period of days to weeks in cats (Henriksson et al., 1961; Collins and Updegraff, 1965; Jeannerod et al., 1976; Clément et al., 1981) and dogs (Collins and Updegraff, 1965) and a period of months in monkeys (Jäger and Henn, 1981a) and humans (Collins, 1964b; Jäger and Henn, 1981b). In order to study dishabituation in goldfish, goldfish were retested at 0.01 Hz at various time intervals following habituation at that frequency. During the interim the goldfish were allowed to swim freely in their home aquaria and kept on alternating 12 h periods of light and dark (see Methods). Gain at 0.01 Hz remained low in three goldfish that were retested two days after habituation. In four goldfish retested after one week, gain at 0.01 Hz recovered nearly half (44%) of its naïve value. Five goldfish were retested at intervals ranging from 1.5 to 10 months after habituation. Four of these had gains higher than in the naïve state, indicating complete dishabituation.

Reexposure to 0.01 Hz rotation caused the VOR to rehabituate in the dishabituated goldfish. The time course of rehabituation was not always shorter than that of the initial habituation. Nor did the time course of rehabituation necessarily resemble that of the initial habituation in terms of the rate of habituation or in the nonlinear and nonstationary aspects of the VOR response. An example of how the time courses of initial habituation can differ is given for goldfish 113 in Fig. 2. Thus, rehabituation was just as variable and unpredictable as initial habituation.

Asymmetrical habituation is associated with a baseline shift in the direction opposite to the habituating half-cycle. Although previous work shows that the habituated state is strongly dependent on the nature of VOR stimulation (Dow and Anastasio, 1996), it might be possible that this baseline shift would persist as a spontaneous nystagmus after the habituating stimulus was terminated.

This possibility was examined in six of the goldfish as they were rehabituating. When the goldfish were exhibiting asymmetrical habituation at 0.01 Hz the stimulus was terminated. In two goldfish, there was a temporary spontaneous nystagmus in the nonhabituated direction. The duration of this spontaneous nystagmus was brief (100 s) in one goldfish, but it persisted for about 400 s in the other. When sinusoidal rotation was resumed, the goldfish immediately returned to their previous level and direction of asymmetrical habituation.

Electrical Stimulations in the Vestibulocerebellum

Previous work in mammals has shown that parts of the cerebellum, particularly the nodulus and uvula, are necessary for habituation to be initiated and maintained (Waespe et al., 1985; Cohen et al., 1992a,

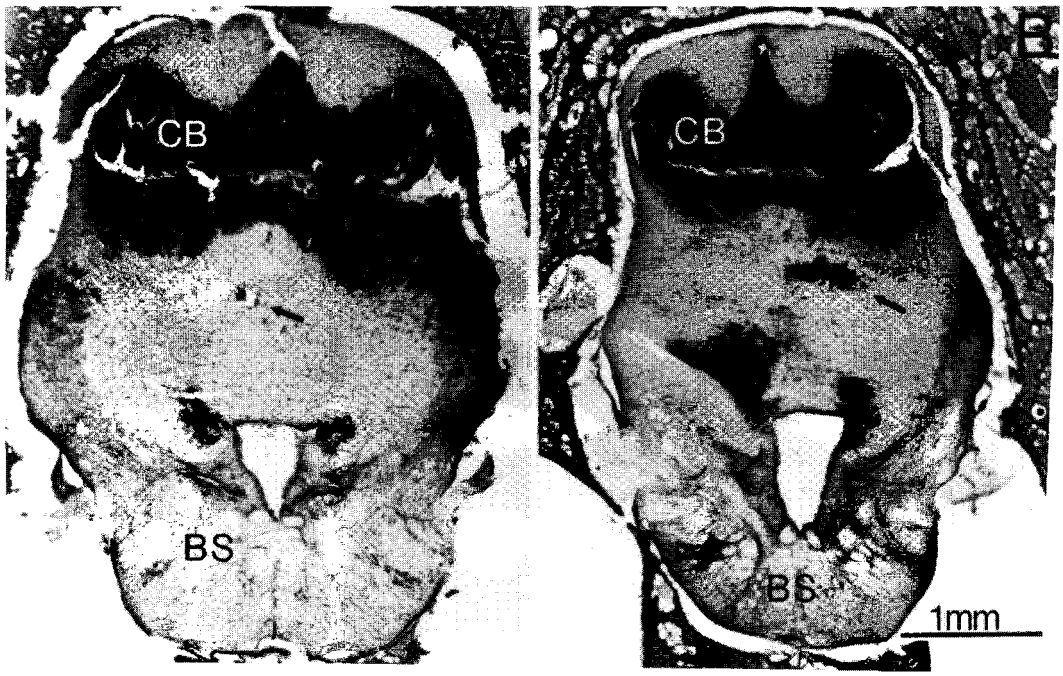

Figure 5. Histological recovery of electrical stimulation and lidocaine injection sites in the vestibulocerebellum of the goldfish. Coronal sections were cut at 50 μm and stained with neutral red. A: Electrical stimulation site was marked by an electrolytic lesion (arrow). Data from this goldfish are shown in Fig. 6. B: The lidocaine injection site was marked with alcian blue dye (arrow) that was dissolved in the lidocaine solution. Data from this goldfish are shown in Fig. 7. The dye spot spread about 500 μm rostral-caudally. CB, cerebellum; BS, brain stem.

1992b; Torte et al., 1994; Angelaki and Hess, 1994). Vestibulocerebellectomy produces dishabituation of the VOR in goldfish (Dow and Anastasio, 1996). It is possible that the vestibulocerebellum produces habituation by directly suppressing the VOR. To explore this possibility, the effects on the VOR of electrical stimulation of the vestibulocerebellum were studied in goldfish. The vestibulocerebellum is located posterior to the main body of the cerebellum in goldfish (Pastor et al., 1994a, 1994b). In order to electrically stimulate the vestibulocerebellum, a metal microelectrode was inserted into it semistereotaxically (see Methods). Following stimulation the site was marked with an electrolytic lesion. Histological recovery of an electrolytic lesion in the Purkinje cell layer of the vestibulocerebellum in a goldfish is shown in Fig. 5A. Electrical stimulation at this site consisted of a 4 s train of bipolar current pulses, 1 ms in width, delivered at a rate of 200/s with an amplitude of ± 60 μA. This stimulation produced complete suppression of an ongoing VOR response to a 0.1 Hz rotation, as shown in Fig. 6. This finding confirms in goldfish a result previously reported in mammals—that stimulation of the vestibulocerebellum can produce suppression of the VOR (Fernández and Fredrickson, 1964; Solomon and Cohen, 1994; see Discussion). This VOR suppression probably occurs through Purkinje cell inhibition of vestibular nuclei neurons.

Lidocaine Injections in the Vestibulocerebellum

The effects on the habituated VOR of temporary lesions of the vestibulocerebellum were studied using microinjections of lidocaine. A mocropipette was inserted into the vestibulocerebellum using the same semistereotaxic procedure used to insert metal microelectrodes, and 250 nl of a 2% lidocaine solution was pressure injected at the site. The injection site was marked for histological recovery with alcian blue dye that was dissolved in the lidocaine solution.

Histological recovery of an injection site is shown in Fig. 5B. The site was located off the midline in the Purkinje cell layer of the vestibulocerebellum. The effects of this injection on the VOR are shown in Fig. 7. Fig. 7A and 7B illustrate naïve and habituated VOR responses, respectively, and lidocaine injection which produced dishabituation. For 15 min postinjection a strong nasal-only response was observed,

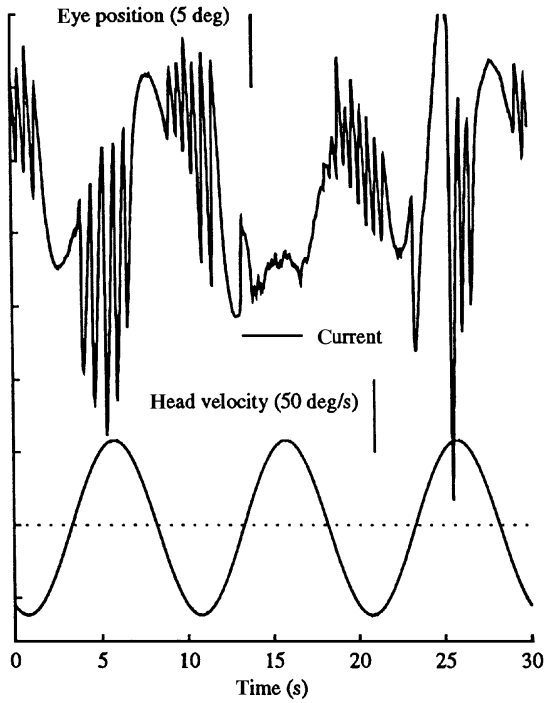

Figure 6. VOR suppression by electrical stimulation of the vestibulocerebellum in a goldfish. The goldfish was rotated at 0.1 Hz, a frequency where habituation is minimal. The eye position trace shows a vigorous response to both directions of head rotation. Stimulation consisted of an alternating electrical current of $\pm 60\ \mu$A. (Stimulation site shown in Fig. 5A.) The nasal response was suppressed for the 4 s duration of the stimulation and resumed shortly after the stimulation ceased.

as shown in Fig. 7C. This is consistent with the laterality of the injection site, since temporary lesion of the left vestibulocerebellum should release the left vestibular nuclei from inhibition, which in turn should allow nasally directed rotation of the left eye (see Fig. 8 for a schematic of the VOR). Head rotation was temporarily stopped (for 6 min) and then resumed in Fig. 7D. The first complete cycle showed a reasonably strong response in both directions. There was slight, abrupt response reduction occurring at $t = 20$ s. The second cycle showed little response, except for a small peak at the onset of the nasal response. The third cycle (and following five cycles, not shown) consisted of a strong temporal response with no nasal response. The asymmetrical, dishabituated response was gradually reduced, and the VOR returned to the habituated state after almost 2 h, as shown in Fig. 7E. In three additional habituated goldfish, a temporary, asymmetrical dishabituation was also induced following lidocaine injection into the vestibulocerebellum (data not shown).

These results show that lidocaine injections into the goldfish vestibulocerebellum produce a temporary dishabituation. Asymmetry in the VOR response postinjection was probably due to uneven spread of lidocaine over the two sides of the cerebellum but could also reflect asymmetry in the response as observed in normal, habituating goldfish. Because cerebellectomy produces dishabituation in goldfish, the fact that the VOR returned to a habituated state after the injection indicates that the injection did not cause significant damage to the vestibulocerebellum. The results suggest the possibility that the lidocaine produced dishabituation by inactivating the Purkinje cells that mediate habituation, and the habituated state returned after the lidocaine wore off. However, the results do not preclude the possibility that the lidocaine produced a dishabituation by some other mechanism, and the habituated state returned after the VOR rehabituated.

Model

The results presented above demonstrate that the VOR response in habituating goldfish was nonlinear and nonstationary in many respects. The xy plot analysis revealed several distinct profiles that characterize these responses, including the soft dead-zone, figure-eight, and crescent (soft rectification). Although these profiles seem disparate, they represent phenomena that were all associated with habituation of the VOR in goldfish. A neural network model of the VOR was constructed to reproduce and unify these results. It is a bilateral model based on the three-neuron-arc of the VOR. The main assumption of the model, which is supported by the results of the electrical stimulation and lidocaine injection experiments, is that the vestibulocerebellum mediates habituation, perhaps through inhibition of vestibular nuclei neurons by Purkinje cells. The purpose of the model is to simulate the nonlinear and nonstationary correlates of VOR habituation. Because VOR habituation occurs only at low frequency, and because previous work (Dow and Anastasio, 1996) shows that habituation switches off when the VOR is exposed to higher-frequency stimulation ($> \sim 0.1$ Hz), the model will focus exclusively on low frequency responses.

The VOR was modeled as a three layer (input, hidden, and output), feedforward neural network similar to that used in previous models of VOR (e.g., Anastasio and Robinson, 1989). In order to focus on the static aspects of VOR responses at various stages of

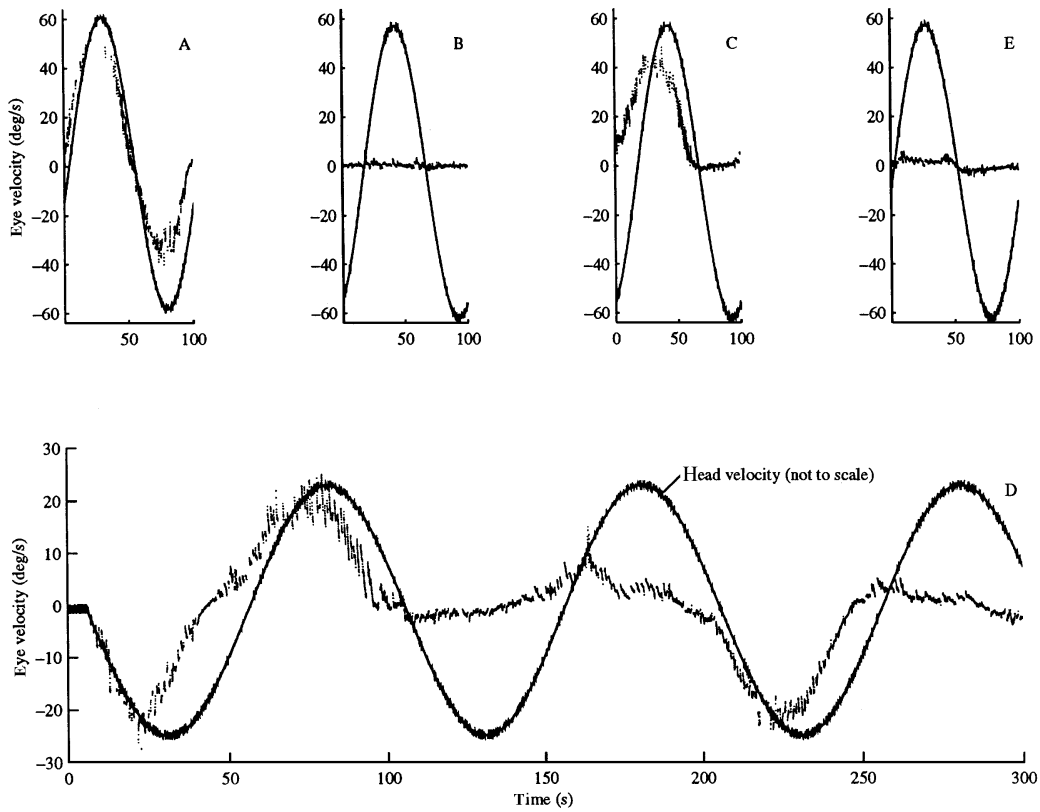

Figure 7. Temporary VOR dishabituation by lidocaine injection off the midline in the vestibulocerebellum of habituated goldfish. All plots show eye and head velocity during 0.01 Hz rotation (head velocity not to scale; peak head velocity 60 deg/s). A: Initial VOR showing strong nasal response and a weaker temporal response. B: VOR following habituation and immediately preceding lidocaine injection. The lidocaine injection was centered about 0.3 mm off the midline on the left side. (Injection site shown in Fig. 5B). C: VOR immediately postinjection showing a nasal-only response for 15 min at which point the rotation was stopped for 6 min. D: Head rotation was resumed about 10 s into D with an immediate response in both directions for one cycle, a slight nasal-only response for the next cycle, followed by a strong temporal-only response for six cycles (only one cycle shown). E: VOR habituation resumes after the lidocaine wears off (almost 2 h postinjection).

habituation, commissural connections between the vestibular nuclei, which influence the dynamics of the VOR, have not been included. The model is schematized in Fig. 8. The left and right vestibular nuclei neurons (*lvn* and *rvn*) were reciprocally innervated by the left and right horizontal canal afferents (*lhc* and *rhc*), such that each vestibular neuron was excited and inhibited by the canal afferent on its ipsilateral and contralateral side, respectively. Each vestibular neuron also received an inhibitory projection from the ipsilateral Purkinje cell (*lpc* and *rpc*) as observed in many species (see Discussion). The vestibular neurons in turn reciprocally innervated the lateral and medial rectus motoneurons (*lr* and *mr*) of the left eye. The vestibular neuron projections were crossed so that the simulated motor commands would produce eye rotation opposite to head rotation.

The neurons in the model computed the weighted sum of their inputs (x) and passed the result through the sigmoidal squashing function [$x' = 1/(1 + e^{-x})$] (Rumelhart et al., 1986). As such, the output of each model neuron, which represented its firing rate, was nonlinearly bounded between 0 and 1. The sigmoidal squashing function has an approximately linear region around 0.5, which is the output of the function (x') when its input (x) equals 0. However, the slope (gain) of the sigmoid gradually decreases and approaches 0 as its output decreases below about 0.25 and increases above about 0.75.

The vestibular neuron to motoneuron weights were arbitrarily assigned the absolute value of 1. The afferent to vestibular neuron weights were set so that the vestibular neurons would have a higher a sensitivity and a lower resting rate than the afferents, as observed

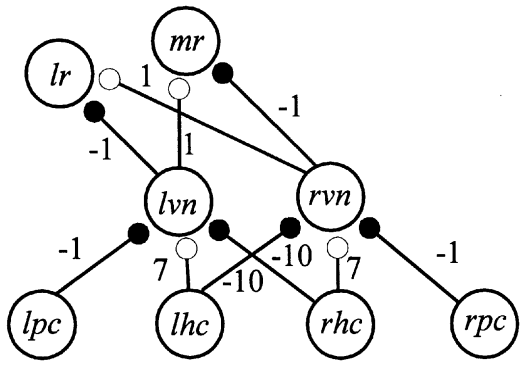

Figure 8. Neural network model of the horizontal VOR. The feedforward network had three layers and was arranged bilaterally. The left and right vestibular nuclei neurons (*lvn* and *rvn*) were reciprocally innervated by the left and right horizontal canal afferents (*lhc* and *rhc*) and were inhibited by the left or right Purkinje cell (*lpc* and *rpc*) on the ipsilateral side. The vestibular neurons in turn reciprocally innervated the lateral rectus and medial rectus (*lr* and *mr*) extraocular muscle motoneurons of the left eye. Filled and open circles represent inhibitory and excitatory connections, respectively. Numbers near the connections indicate the values of the connection weights. Only the Purkinje cell firing rates were varied in the simulations.

experimentally in goldfish (Allum et al., 1976; Allum and Graf, 1977; Hartmann and Klinke, 1980). The sensitivity of the vestibular neurons was enhanced by making the absolute values of the afferent to vestibular neuron weights relatively large. The resting rate of the vestibular neurons was lowered by making the absolute values of the contralateral, inhibitory afferent weights larger than those of the ipsilateral, excitatory afferent weights. The weight of the connection from each Purkinje cell to the ipsilateral vestibular neuron was set at -1, and all of the weights in the network were balanced bilaterally. The values of the weights were fixed for all simulations as indicated in Fig. 8. Only the activities of the Purkinje cells were varied.

Simulations of a naïve response and an abrupt-onset response reduction are illustrated in Fig. 9. Figure 9A shows the time series of the responses of the neurons in the network. Because the network is arranged to work in push-pull, the responses of the two afferents differ only by a rotation about the response equals 0.5 axis, and likewise for the two motoneurons. Therefore, the responses of only one each of the afferents (*lhc*) and the motoneurons (*mr*) are shown. However, the vestibular neurons can be affected asymmetrically by the Purkinje cells, so the responses of both (*lvn* and *rvn*) are shown. To simulate a head rotation at 0.01 Hz, the firing rates of the afferents are modulated sinusoidally (and in push-pull) at that frequency, about a resting rate of 0.5. To keep the afferent activity sinusoidal, the afferents were modulated in the approximately linear range of the sigmoidal squashing function.

The network was run in the naïve state for the first 225 s of the simulation. (Each time step in the simulations corresponded to 0.5 s.) In the naïve network, when Purkinje cell firing rate is 0 on both sides, both vestibular neurons respond identically except for a half-cycle of phase difference between them. The vestibular neuron responses during the inhibitory half-cycle are slightly distorted because they fall in the lower nonlinear range of the sigmoidal squashing function. However, this symmetrical distortion is canceled out at the motoneurons, due to their reciprocal connections from the vestibular neurons. In the naïve state, the firing rates of the motoneurons are modulated sinusoidally (and in push-pull) at the stimulus frequency, about a resting rate of 0.5. This motoneuron command would produce a sinusoidal VOR eye velocity response at a frequency of 0.01 Hz.

To compare the behavior of the model with that of the goldfish VOR, model xy plots were constructed by plotting the response of motoneuron *mr* against that of afferent *lhc*. This was equivalent to the VOR xy plots because the motoneuron and afferent responses represented eye and head velocity in the model. As for the experimental VOR data, the responses of *mr* and *lhc* in the model were shifted in time to minimize any phase difference between them before the xy plots were made. The xy plot for the model in the naïve state is shown in Fig. 9B. Because both the afferent and motoneuron responses are sinusoidal, the xy plot is a straight line. This xy plot can be compared with that for the naïve VOR shown in Fig. 3A, which is also roughly a straight line.

The model was used to simulate an abrupt reduction in the VOR response. This type of nonstationarity was frequently observed during VOR habituation in goldfish, and occurred at or near peak eye velocity (e.g., Fig. 2). It was simulated by changing the firing rate of the Purkinje cell on one side, in one time step, at the peak of the motoneuron response. Starting at $t = 225$ s, the firing rate of the left Purkinje cell (*lpc*) was changed from 0 to 3.5 while that of the right Purkinje cell (*rpc*) remained at 0. This produced an abrupt reduction in the response of *lvn* but did not affect the response of *rvn* (Fig. 9A). Because the motoneurons essentially were now driven only by one vestibular neuron (*rvn*), their response amplitude was abruptly

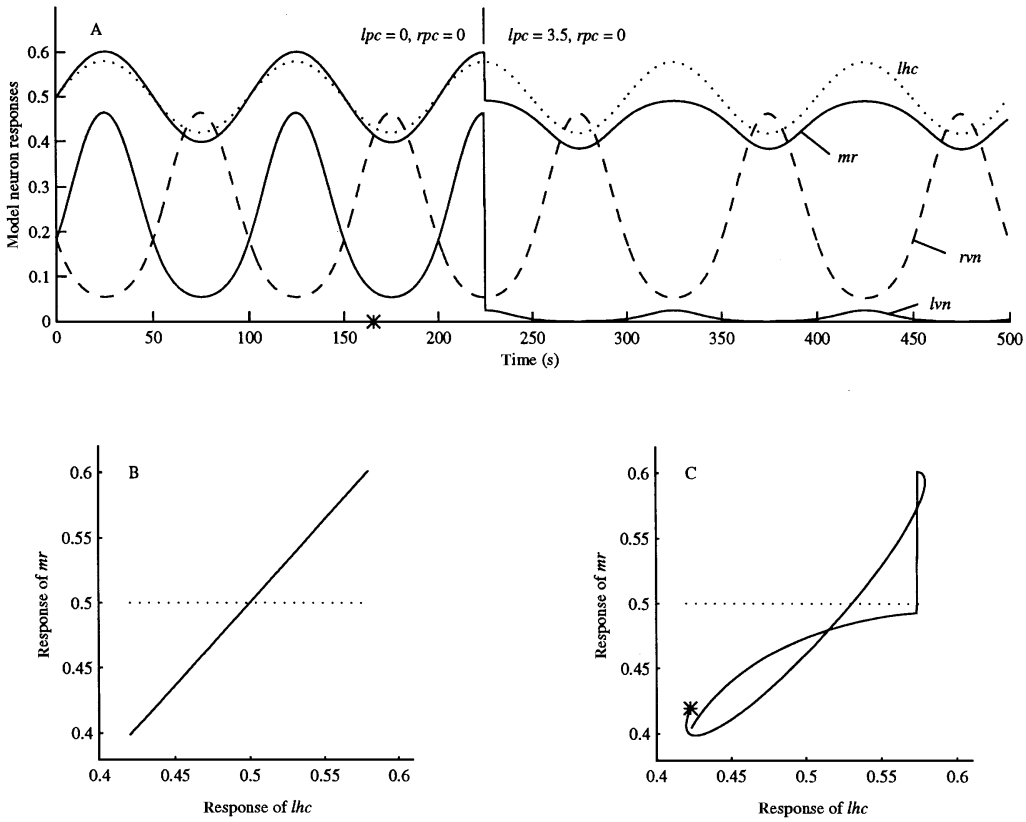

Figure 9. Neural network simulation of the VOR showing the naïve response and an abrupt-onset habituation. A: Simulated responses of the left horizontal canal afferent (*lhc*), the vestibular nuclei reurons (*lvn* and *rvn*), and the medial rectus motoneuron (*mr*) at 0.01 Hz. The responses of *lhc* and *mr* represent head and VOR eye velocity, respectively. The vestibular neurons had a lower spontaneous rate and higher sensitivity than the afferents. Between $t = 0$ and $t = 225$ s, both Purkinje cells were inactive and the motoneuron response is strong and linear. B: The linear response is shown in an xy plot, which can be compared to the data in Fig. 3A. At $t = 225$ s, the left Purkinje cell (*lpc*) became active and immediately inhibited *lvn*, suppressing its response; *rvn* is not inhibited. C: The affect of this abrupt-onset inhibition is shown in the figure-eight xy plot, which can be compared to the data in Fig. 3C. The asterisk in C shows the beginning of the trace as also marked in A.

reduced, and the response reflected the distortion inherent in the individual vestibular neuron response.

An xy plot was constructed from the response cycle that spanned the abrupt response reduction and is shown in Fig. 9C (the asterisk marks the beginning of the cycle in Figs. 9A and 9C). The half-cycle before the nonstationarity has an elliptical xy trajectory, due to a small phase difference introduced into the first half-cycle by minimizing the phase difference of the whole cycle of the response. The nonstationarity produces a disctontinuity in the xy trajectory as the response of *mr* is abruptly reduced. In the half-cycle following the nonstationarity, the xy trajectory crosses itself once as it returns near to its beginning point with a crescent-shaped profile. The overall effect of the abrupt response reduction occurring at the peak is a figure-eight xy profile that is comparable to that produced from nonstationary experimental data (Fig. 3C). Although the VOR network model, with sigmoidal, nonlinear model neurons, was capable of producing a variety of xy profiles (see below), trajectories that crossed themselves as in the figure-eight could be produced only with a nonstationary change in response amplitude occurring within the cycle. The crescent-shaped segment of the figure-eight xy profiles, both for model and experimental data, was due to response asymmetry.

Stationary but asymmetrical responses were simulated by setting the Purkinje cell inhibition of the vestibular neurons on both sides to values that were nonzero but unequal. The actual values of these firing rates were chosen to provide a good match between the xy plots constructed from model and experimental

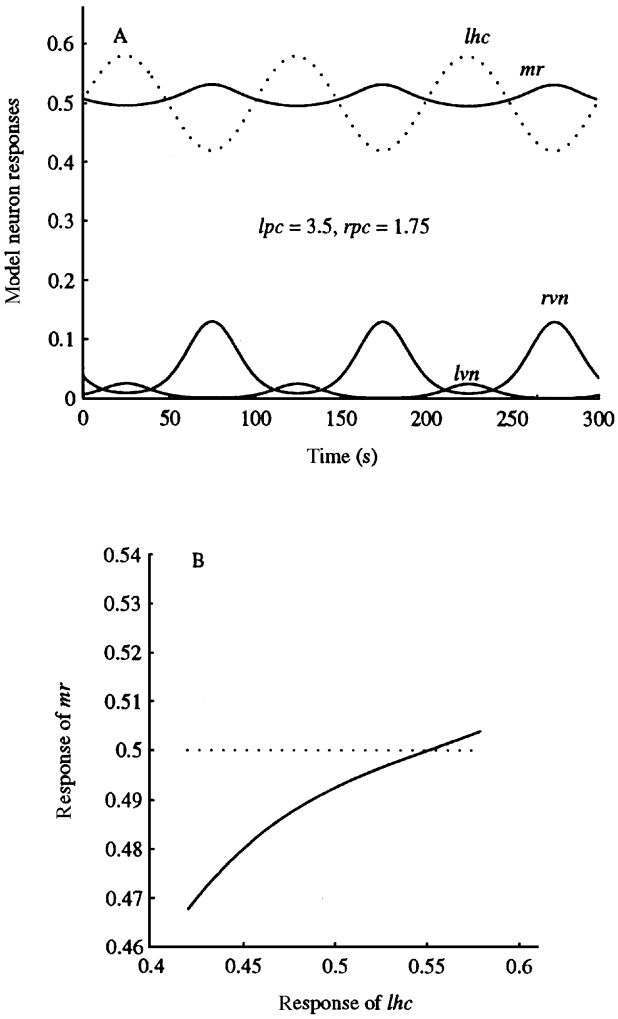

Figure 10. Neural network simulation of asymmetrical VOR habituation. A: Simulated neural responses due to asymmetrical inhibition from the Purkinje cells (*lpc* and *rpc*). The left vestibular neuron (*lvn*) responded only at the peak of the left afferent input, while the right vestibular neuron (*rvn*) responded throughout the upper half cycle of the right afferent input. B: The resulting crescent (soft rectification) *xy* plot can be compared to the data in Figs. 3D and 3E.

data. For the example shown in Fig. 10, the firing rates of *lpc* and *rpc* were set at 3.5 and 1.75, respectively. This reduced the response of *lvn* more than that of *rvn* (Fig. 10A). As in the previous case after the nonstationarity, the motoneurons in the stationary but asymmetrical case essentially were driven only by *rvn*. They have a reduced response amplitude, and the response also reflects the distortion inherent in the individual vestibular neuron response. This response distortion can be characterized as a flattening or soft-rectification in the time series for the response in one direction and is apparent both for model and experimental data (Fig. 2). Note that the baseline of the *mr* response has shifted up (from 0.5) in the direction of the more strongly responding half-cycle. Similar baseline shifts are apparent in the experimental data during asymmetrical habituation (Fig. 2). In the model, the baseline shift occurs because unequal Purkinje cell inhibition causes an imbalance in activity at the vestibular nuclei level. If it persisted in the absence of rotation, this imbalance would produce a spontaneous nystagmus. Spontaneous nystagmus was observed in some cases after sinusoidal rotation was terminated during asymmetrical habituation (see above). The asymmetry of the response of *mr* produces a crescent-shaped *xy* profile (Fig. 10B) that is comparable to that produced from asymmetrical experimental data (Figs. 3D and 3E).

Magnitude dependency was simulated by setting the Purkinje cell firing rate to some relatively high value that was equal on both sides. Again, the actual values were chosen to provide a good approximation to the experimental data. In the example shown in Fig. 11, the firing rates of *rpc* and *lpc* were both set to 3.5. The firing rate of the afferents in this example were modulated at 0.03 Hz because magnitude dependency in the VOR was most often observed at frequencies that were slightly higher than 0.01 Hz. To reflect the fact that afferent gain is about three times higher at 0.03 Hz than at 0.01 Hz in goldfish (Hartmann and Klinke, 1980), the depth of the modulation of the afferent response was increased three times. The responses of the vestibular neurons were severely distorted in this case (Fig. 11A). The high Purkinje cell inhibition caused them to rectify for the half-cycle in their inhibitory direction and caused the response for the excitatory half-cycle to occur in the lower nonlinear region of the sigmoidal squashing function. This is the region in which the sigmoid sweeps up from a very low gain, where the firing rate is near 0 (rectified), and into the higher gain region. Thus, with strong bilateral Purkinje cell inhibition, the responses of the vestibular neurons were weak as they came out of rectification, but then peaked sharply. The result of this at the motoneuron level was a magnitude-dependent response that was stronger at the peaks than midrange. This produced a soft deadzone *xy* profile (Fig. 11B) that is comparable to that produced from VOR data in goldfish, particularly at a frequency slightly higher than the habituating frequency (Fig. 4).

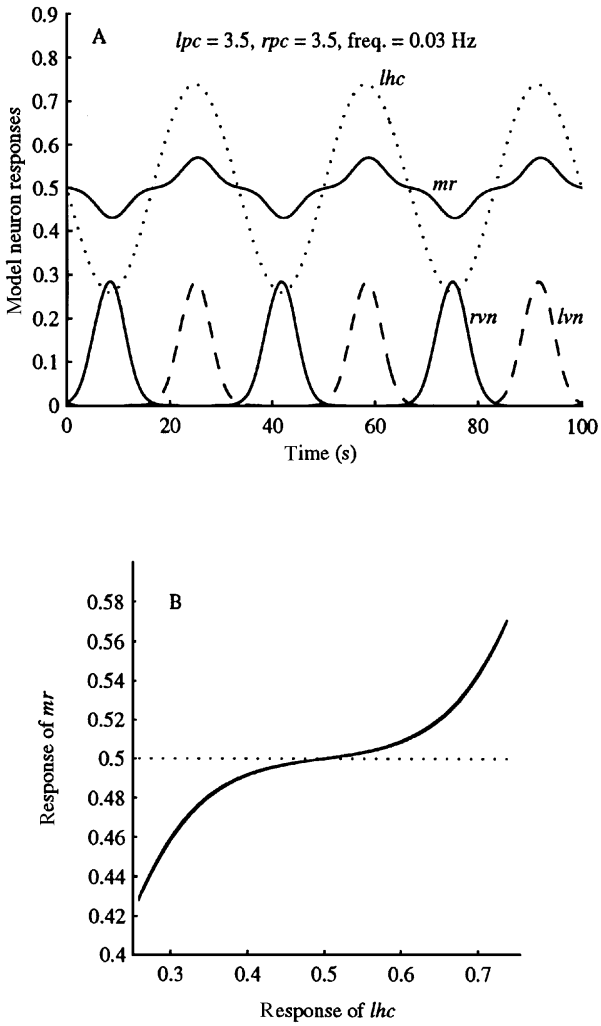

Figure 11. Neural network simulation of a VOR dead-zone nonlinearity following habituation. The frequency was increased to 0.03 Hz. The afferent input (*lhc*) was also increased three times to model the increase in frequency-dependent gain of the canal afferents in going from 0.01 to 0.03 Hz. The Purkinje cells (*lpc* and *rpc*) were both equally active, providing strong and symmetrical inhibition of the vestibular neurons (*lvn* and *rvn*), which responded to the afferent input much more strongly at the peaks than midrange. A: Model neuron responses. B: The resulting soft dead-zone *xy* plot can be compared to the data in Fig. 4.

As Purkinje cell inhibition was further increased, the responses at the vestibular neuron and motoneuron levels decrease until they become essentially flat. This resulted in a flat *xy* profile (not shown), which was also produced from the VOR response at an advanced stage of habituation (Fig. 3F). Thus, this simple VOR neural network model was capable of reproducing all of the nonlinear and nonstationary *xy* profiles that were observed for the VOR in habituating and habituated goldfish, and it did so by changing only the firing rates of the Purkinje cells that were inhibitory to the vestibular neurons in the model.

Discussion

Prolonged sinusoidal head rotation at a low frequency in the dark causes VOR gain at that frequency to go down in goldfish (Dow and Anastasio, 1996). This has also been observed in cats (Clément et al., 1981), rats (Tempia et al., 1991), monkeys (Buettner et al., 1981; Jäger and Henn, 1981a, 1981b), and humans (Jäger and Henn, 1981b). Previous work suggests that VOR habituation is associated with nonstationarities and nonlinearities. In a recent study in goldfish (Dow and Anastasio, 1996), VOR gain was first habituated by continued rotation at 0.01 Hz, but then the gain at that frequency was found to increase 20 times when the 0.01 Hz rotation was combined with a 0.3 Hz rotation. Thus, VOR gain at a low, habituated frequency in goldfish depended on whether rotation at that frequency was presented alone or combined with a higher-frequency rotation. This finding demonstrated that the VOR in habituated goldfish is nonlinear in that it fails to obey the superposition principle of linear systems. The 0.01 Hz gain returned to its habituated value immediately after the 0.3 Hz component was removed. This suggested that some nonstationary mechanism switched in to reduce VOR gain at low but not high frequency in habituated goldfish. Nonstationary and nonlinear behavior associated with habituation has been reported in the rat, including rapid onset and asymmetry of habituation of the VOR (Tempia et al., 1991). Habituation in goldfish is associated with similar nonstationary and nonlinear VOR response characteristics.

It has been shown in higher mammals that VOR gain is correlated with arousal level (Crampton and Schwam, 1961; Collins et al., 1964b; Paige, 1983; Tempia et al., 1991). However, it is very unlikely that the VOR gain reductions described here are related to decreases in arousal. For example, it could be argued that VOR gain is high at first and then decreases as arousal decreases during prolonged rotation at 0.01 Hz. If this were the case, then arousing the goldfish by stopping and restarting rotation at 0.01 Hz should restore VOR gain, but this was never observed. In dishabituation experiments, VOR gain was measured, from the start of 0.01 Hz rotation, to be at its low, habituated level even one or more days after the initial habituation.

Previous work (Dow and Anastasio, 1996) shows that the gain at 0.01 Hz immediately returns to its low, habituated value when a higher-frequency component is removed from the stimulus. It is very unlikely that the gain decrease observed here is due to an immediate decrease in arousal—brought about by removing the higher-frequency stimulus component—that is sufficient to reduce the VOR gain by 20 times. Instead, these results support the view that habituation, which reduces low-frequency VOR gain, can persist over days but can be modulated by higher-frequency stimulation.

Analysis of time series during VOR habituation in goldfish revealed several nonlinear and nonstationary features that included asymmetries, magnitude dependencies, and abrupt transitions. Reduction in the amplitude of the VOR response at 0.01 Hz often began during the first cycle of rotation at that frequency in goldfish. Reduction in the amplitude of the VOR response at 0.05 Hz in rat could begin after the first several cycles (Tempia et al., 1991). Although habituation appeared to proceed smoothly in the rat, reductions in VOR response amplitude during habituation could be abrupt in goldfish. These abrupt transitions are also suggestive of a switching mechanism. The most frequently observed nonlinearity observed during habituation in goldfish was asymmetry in the VOR response. This asymmetry consisted of a decrease in the amplitude of the VOR response that was unequal for the two directions of rotation. Asymmetries have also been observed in the rat VOR as it habituated to sinusoidal stimulation at 0.05 Hz (Tempia et al., 1991). Asymmetrical habituation that was direction specific was produced in the cat with repeated unilateral transient rotations (Crampton, 1962; Collins, 1964a; Clément et al., 1981).

The neural substrates of the nonlinear and nonstationary behavior exhibited by the VOR during habituation probably include processes occurring in the vestibular nuclei and parts of the vestibulocerebellum. Although the responses of vestibular afferents do not appear to habituate (Proctor and Fernández, 1963; Courjon et al., 1987), the responses of vestibular nuclei neurons have been observed to decrease with repeated transient rotations, possibly to the point of cutoff (Kileny et al., 1980). This suggests that habituation of the VOR involves a reduction in the response of vestibular nuclei neurons. Lesions in the nodulus and uvula of the vestibulocerebellum produce dishabituation in the cat (Singleton, 1967; Torte et al., 1994) and monkey (Waespe et al., 1985; Cohen et al., 1992a, 1992b). Cerebellectomy also produces permanent dishabituation in goldfish (Dow and Anastasio, 1996). Injections of lidocaine into the goldfish vestibulocerebellum produce a temporary dishabituation, while electrical stimulation in the vestibulocerebellum can suppress the VOR in goldfish (see Results). Electrical stimulation of the nodulus also produces suppression of the VOR in the cat (Fernández and Fredrickson, 1964) and monkey (Solomon and Cohen, 1994). These findings support the hypothesis that the vestibulocerebellum produces habituation, presumably through Purkinje cell inhibition of vestibular nuclei neurons.

Purkinje cells in the vestibulocerebellum project to the vestibular nuclei in all vertebrates (Butler and Hodos, 1996). Purkinje cells of the nodulus and uvula project to the ipsilateral vestibular nuclei in many mammals including the rat (Dow, 1936; Achenbach and Goodman, 1968), cat (Dow, 1936; Angaut and Brodal, 1967; Precht et al., 1976; Ito et al., 1982; Carleton and Carpenter, 1983; Carpenter and Cowie, 1985; Shojaku et al., 1987), albino rabbit (Balaban, 1984), and monkey (Dow, 1938; Carleton and Carpenter, 1983). Pastor and Colleagues (1994a) have identified inhibitory vestibulocerebellar projections to a group of 25 to 40 premotor neurons in the brainstem of the goldfish that provide a necessary velocity signal to the vestibular nuclei. Thus, Purkinje cells in goldfish can directly suppress the ipsilateral vestibular nuclei neurons.

The above hypothesis and anatomical data were incorporated into a neural network model of the VOR. The model contained neurons that had sigmoidal input/output functions. This nonlinear function is widely used to model the summed output of subpopulations of neurons that have different thresholds and saturation points and process similar inputs in parallel (Rumelhart et al., 1986). The sigmoid is therefore an appropriate nonlinearity to use to model the neurons at the three bilateral stages of the VOR. Although the nonlinearity of the individual vestibular neurons is a simple sigmoid, the network can reproduce all of the nonlinear and nonstationary features of the VOR in habituating goldfish by combining the outputs of those vestibular neurons as their resting rates along the sigmoid are shifted by differing levels of Purkinje cell inhibition. These features were characterized by input/output functions, revealed as xy plot profiles, that included the figure-eight for the abrupt decrease in amplitude, the soft rectification (crescent) for the asymmetrical response, and the soft dead-zone for the magnitude-dependent response. Thus, the model demonstrates that the variety

of nonlinear behaviors observed for the overall VOR during habituation may commonly emerge from the essential nonlinearity of the vestibular neurons that mediate it.

Taken together, the experimental and modeling results support the hypothesis that VOR habituation is brought about through the inhibition of vestibular nuclei neurons by Purkinje cells from the vestibulocerebellum. Habituation can cause the VOR to become nonstationary in that the amplitude of its response to low-frequency rotations can be reduced rapidly and sometimes abruptly. The model predicts that during habituation, Purkinje cells responsible for habituation make abrupt changes in their firing rate to suppress the ipsilateral vestibular nuclei. Habituation can also cause the VOR to exhibit nonlinear behaviors such as rectification and magnitude dependency, as habituation unmasks the essential nonlinearity of the vestibular neurons that is usually hidden under naïve conditions.

In the model, asymmetric habituation is simulated by a Purkinje cell inhibition of the vestibular nuclei that is higher on one side than the other. This simulates both the asymmetric response and the associated baseline shift. In the absence of rotation such an imbalance would result in spontaneous nystagmus. A spontaneous nystagmus was observed when sinusoidal rotation was terminated during asymmetrical habituation in two out of six cases. This spontaneous nystagmus lasted for at most 400 s. When rotation was resumed, the goldfish continued to display asymmetrical habituation in the same direction and at the same reduced gain. The finding suggests that any imbalance that develops, like habituation itself, is sensitive to rotational frequency and that cerebellar inhibition quickly decreases when rotation at that frequency is terminated. Spontaneous nystagmus was never observed at the end of 1 h of rotation and would not have been expected because the response was always strongly attenuated in both directions.

The results also shed some light on the nature of adaptive learning in the VOR. The time series analysis shows that the time course of VOR habituation (Fig. 2) is asymmetrical and exhibits abrupt transitions and reversals. These features are best characterized as a switching nonstationarity. They are inconsistent with an error-driven learning hypothesis for VOR habituation, in which the target VOR gain for low-frequency stimulation would be 0, and VOR gain would decrease to 0 exponentially in proportion to its current error.

The experimental results and simulations support the view that habituation is mediated by parts of the vestibulocerebellum. Vestibular afferents and vestibular nuclei neurons project to the vestibulocerebellum as mossy fibers (Llinás and Walton, 1990). The vestibular input is processed by cerebellar interneurons before it affects the activity of Purkinje cells. The end product of that processing is represented in the model simply as changes in an otherwise constant Purkinje cell activity level, which were sufficient to reproduce the nonstationary and nonlinear behavior correlated with VOR habituation. Ongoing modeling work will focus on possible mechanisms of cerebellar processing of vestibular signals. It will address other questions concerning the mechanisms of habituation, such as why VOR habituation is asymmetrical and abrupt, whether a "target" VOR low-frequency gain is actually set, how it is set for habituation or reset for dishabituation, how the frequency specificity of habituation develops, and the effects of this frequency specificity on habituated VOR dynamics.

Acknowledgment

We thank Kristen Dempsey, Amy Durkin, Thomedi Ventura, and Mario Zelaya for technical assistance and Dr. Ehtibar Dzhafarov for consultation on statistics. This work was supported by NIH grant MH50577.

References

Achenbach KE, Goodman DC (1968) Cerebellar projections to pons, medulla, and spinal cord in the albino rat. *Brain Behav. Evol.* 1:43–57.

Allum JHJ, Graf W (1977) Time constants of vestibular nuclei neurons in the goldfish: A model with ocular proprioception. *Biol. Cybern.* 28:95–99.

Allum JHJ, Graf W, Dichgans J, Schmidt CL (1976) Visual-vestibular interactions in the vestibular nuclei of the goldfish. *Exp. Brain Res.* 26:463–485.

Anastasio TJ, Robinson DA (1989) The distributed representation of vestibulo-oculomotor signals by brain-stem neurons. *Biol. Cybern.* 61:79–88.

Angaut P, Brodal A (1967) The projection of the "vestibulocerebellum" onto the vestibular nuclei in the cat. *Arch Ital. Biol.* 105:441–479.

Angelaki DE, Hess BJM (1994) The cerebellar nodulus and ventral uvula control the torsional vestibulo-ocular reflex. *J. Neurophysiol.* 72:1443–1447.

Bahill AT, McDonald JD (1983) Frequency limitations and optimal step size for the two-point central difference derivative algorithm with applications to human eye movement data. *IEEE Trans. Biomed. Eng.* 30:191–194.

Balaban CD (1984) Olivo-vestibular and cerebello-vestibular connections in albino rabbits. *Neurosci.* 12:129–149.

Buettner UW, Henn V, Young LR (1981) Frequency response of the vestibulo-ocular reflex (VOR) in the monkey. *Aviat. Space Environ. Med.* 52:73–77.

Butler AB, Hodos W (1996) Comparative Vertebrate Neuroanatomy: Evolution and Adaptation. John Wiley, New York. p. 194.

Carleton SG, Carpenter MB (1983) Afferent and efferent connections of the medial, inferior, and lateral vestibular nuclei in the cat and monkey. *Brain Res.* 278:29–51.

Carpenter MB, Cowie RJ (1985) Connections and oculomotor projections of the superior vestibular nucleus and cell group "y." *Brain Res.* 336:265–287.

Clément G, Courjon JH, Jeannerod M, Schmid R (1981) Unidirectional habituation of vestibulo-ocular responses by repeated rotational or optokinetic stimulations in the cat. *Exp. Brain Res.* 42:34–42.

Cohen H, Cohen B, Raphan T, Waespe W (1992a) Habituation and adaptation of the vestibuloocular reflex: A model of differential control by the vestibulocerebellum. *Exp. Brain Res.* 90:526–538.

Cohen B, Reisine H, Yokota J, Raphan T (1992b) The nucleus of the optic tract: Its function in gaze stabilization and control of visual-vestibular interaction. In: B Cohen, DL Tomko, F Guedry, eds. Sensing and Controlling Motion: Vestibular and Sensorimotor Function. Annals of the New York Academy of Sciences, New York, vol. 656, pp. 277–296.

Collins WE (1964a) Primary, secondary, and caloric nystagmus of the cat following habituation to rotation. *J. Comp. Physiol. Psychol.* 57:417–421.

Collins WE (1964b) Task-control of arousal and the effects of repeated unidirectional angular acceleration on human vestibular responses. *Acta Otolaryngol. Suppl*. 190:1–34.

Collins WE, Updegraff BP (1965) A comparison of nystagmus habituation in the cat and dog. *Acta Otolaryngol.* 62:19–26.

Courjon JH, Precht W, Sirkin DW (1987) Vestibular nerve and nuclei unit responses and eye movement responses to repetitive galvanic stimulation of the labyrinth in the rat. *Exp. Brain Res.* 66:41–48.

Crampton GH (1962) Directional imbalance of vestibular nystagmus in cat following repeated unidirectional angular acceleration. *Acta Otolaryngol.* 55:41–48.

Crampton GH, Schwam WJ (1961) Effects of arousal reaction on nystagmus habituation in cat. *Am. J. Physiol.* 200:29–33.

Dow RS (1936) The fiber connections of the posterior parts of the cerebellum in the rat and cat. *J. Comp. Neurol.* 63:527–548.

Dow RS (1938) Efferent connections of the flocculo nodular lobe in macaca mulatta. *J. Comp. Neurol.* 68:297–305.

Dow ER, Anastasio TJ (1996) Violation of superposition by the vestibulo-ocular reflex of the goldfish. *Neuroreport* 7:1305–1309.

Fernández C, Fredrickson JM (1964) Experimental cerebellar lesions and their effect on vestibular function. *Acta Otolaryngol. Suppl.* 192:52–62.

Grossman GE, Leigh RJ, Abel LA, Lanska DJ, Thurston SE (1988) Frequency and velocity of rotational head perturbations during locomotion. *Exp. Brain Res.* 70:470–476.

Hartmann R, Klinke R (1980) Discharge properties of afferent fibres of the goldfish semicircular canal with high frequency stimulation. *Pflügers Arch.* 388:111–121.

Henriksson NG, Kohut R, Fernández C (1961) Studies on habituation of vestibular reflexes. *Acta Otolaryng.* 53:333–349.

Ito M, Shiida T, Yagi N, Yamamoto M (1974) Visual influence on rabbit horizontal vestibulo-ocular reflex presumably effected via the cerebellar flocculus. *Brain Res.* 65:170–174.

Ito J, Sasa M, Matsuoka I, Takaori S (1982) Afferent projection from reticular nuclei, inferior olive and cerebellum to lateral vestibular nucleus of the cat as demonstrated by horseradish peroxidase. *Brain Res.* 231:427–432.

Jäger J, Henn V (1981a) Habituation of the vestibulo-ocular reflex (VOR) in the monkey during sinusoidal rotation in the dark. *Exp. Brain Res.* 41:108–114.

Jäger J, Henn V (1981b) Vestibular habituation in man and monkey during sinusoidal rotation. In: B Cohen, ed. Vestibular and Oculomotor Physiology: International Meeting of the Bárány Society. New York Acadamy of Sciences, New York. vol. 374. pp. 330–339.

Jeannerod M, Clement G, Courjon JH, Schmid R (1981) Unilateral habituation of vestibulo-ocular responses in the cat. In: Cohen B, ed. Vestibular and Oculomotor Physiology: International Meeting of the Bárány Society. New York Acadamy of Sciences, New York. vol. 374. pp. 340–351.

Jeannerod M, Magnin M, Schmid R, Stefanelli M (1976) Vestibular habituation to angular velocity steps in the cat. *Biol. Cybern.* 22:39–48.

Kileny P, Ryu JH, McCabe BF, Abbas PJ (1980) Neuronal habituation in the vestibular nuclei of the cat. *Acta Otolaryngol.* 90:175–183.

Kleinschmidt HJ, Collewijn H (1975) A search for habituation of vestibulo-ocular reactions to rotary and linear sinusoidal accelerations in the rabbit. *Exp. Neurol.* 47:257–267.

Llinás RR, Walton KD (1990) Cerebellum. In: GM Shepherd, ed. The Synaptic Organization of the Brain. Oxford University Press, New York, pp. 214–245.

Mertens RA, Collins WE (1967) Unilateral caloric habituation of nystagmus in the cat: Effects on rotational and bilateral caloric responses. *Acta Otolaryngol.* 64:281–297.

Paige G. (1983) VOR and its interaction with visual following mechanisms in the squirrel monkey: I. Response characteristics in normal animals. *J. Neurophysiol.* 49:134–151.

Pastor AM, de la Cruz RR, Baker R (1992) Characterization and adaptive modification of the goldfish vestibulo-ocular reflex by sinusoidal and velocity step vestibular stimulation in the goldfish. *J. Neurophysiol.* 68:2003–2015.

Pastor AM, de la Cruz RR, Baker R (1994a) Cerebellar role in adaptation of the goldfish vestibuloocular reflex. *J. Neurophysiol.* 72:1383–1394.

Pastor AM, de la Cruz RR, Baker R (1994b) Eye position and eye velocity integrators reside in separate brainstem nuclei. *Proc. Natl. Acad. Sci. USA* 91:807–811.

Precht W, Volkind R, Maeda M, Giretti ML (1976) The effects of stimulating the cerebellar nodulus in the cat on the responses of vestibular neurons. *Neurosci.* 1:301–312.

Proctor LR, Fernández C (1963) Studies on habituation of vestibular reflexes: IV. Effect of caloric stimulation in blindfolded cats. *Acta Otolaryngol.* 56:500–508.

Remmel RS (1984) An inexpensive eye movement monitor using the scleral search coil technique. *IEEE Trans. Biomed. Eng.* 31:388–390.

Robinson DA (1963) A method for measuring eye movement using a scleral search coil in a magnetic field. *IEEE Trans. Biomed. Eng.* 10:137–145.

Rumelhart DE, McClelland JL, P.D.P. Research Group (eds.) (1986) Parallel Distributed Processing: Explorations in the Microstructure of Cognition. Vol. 1, Foundations. MIT Press, Cambridge, MA.

Schairer JO, Bennett MVL (1986) Changes in gain of the vestibulo-ocular reflex induced by combined visual and vestibular stimulation in goldfish. *Brain Res.* 373:164–176.

Schmid R, Jeannerod M (1985) Vestibular habituation: An adaptive process? In: A Berthoz, G Melvill-Jones, eds. Adaptive Mechanisms in Gaze Control. Elsevier, New York. vol. 1, pp. 113–122.

Segal BN, Outerbridge JS (1982a) A nonlinear model of semicircular canal primary afferents in bullfrog. *J. Neurophysiol.* 47:563–578.

Segal BN, Outerbridge JS (1982b) Vestibular (semicircular canal) primary neurons in bullfrog: Nonlinearity of individual and population response to rotation. *J. Neurophysiol.* 47:545–562.

Shojaku H, Sato Y, Ikarashi K, Kawasaki T (1987) Topographical distribution of Purkinje cells in the uvula and the nodulus projecting to the vestibular nuclei in cats. *Brain Res.* 416:100–112.

Singleton GT (1967) Relationships of the cerebellar nodulus to vestibular function: A study of the effects of nodulectomy on habituation. *Laryngoscope* 77:1579–1620.

Solomon D, Cohen B (1994) Stimulation of the nodulus and uvula discharges velocity storage in the vestibular-ocular reflex. *Exp. Brain Res.* 102:57–68.

Tempia F, Dieringer N, Strata P (1991) Adaptation and habituation of the vestibulo-ocular reflex in intact and inferior olive-lesioned rats. *Exp. Brain Res.* 86:568–578.

Torte MP, Courjon JH, Flandrin JM, Magnin M, Magenes G (1994) Anatomical segregation of different adaptive processes within the vestibulocerebellum of the cat. *Exp. Brain Res.* 99:441–454.

Waespe W, Cohen B, Raphan T (1985) Dynamic modification of the vestibulo-ocular reflex by the nodulus and uvula. *Science* 228:199–202.

Weissenstein L, Ratnam R, Anastasio TJ (1996) Vestibular compensation in the horizontal vestibulo-ocular reflex of the goldfish. *Behav. Brain Res.* 75:127–137.

Wilson V, Melvill Jones G (1979) Mammalian Vestibular Physiology, Plenum Press, New York.